A Period of Controlled Elevation of IOP (CEI) Produces the Specific Gene Expression Responses and Focal Injury Pattern of Experimental Rat Glaucoma

John C. Morrison,[1] William O. Cepurna,[1] Shandiz Tehrani,[1] Tiffany E. Choe,[1] Hari Jayaram,[1,2] Diana C. Lozano,[1] Brad Fortune,[3] and Elaine C. Johnson[1]

[1]The Kenneth C. Swan Ocular Neurobiology Laboratory, Casey Eye Institute, Oregon Health and Science University, Portland, Oregon, United States
[2]Glaucoma Service, NIHR Moorfields Biomedical Research Centre, London, United Kingdom
[3]Devers Eye Institute, Portland, Oregon, United States

Correspondence: John C. Morrison, Casey Eye Institute, 3375 SW Terwilliger Boulevard, Portland, OR 97239-4197, USA; morrisoj@ohsu.edu.

Submitted: August 19, 2016
Accepted: October 31, 2016

Citation: Morrison JC, Cepurna WO, Tehrani S, et al. A period of controlled elevation of IOP (CEI) produces the specific gene expression responses and focal injury pattern of experimental rat glaucoma. *Invest Ophthalmol Vis Sci*. 2016;57:6700–6711. DOI: 10.1167/iovs.16-20573

Purpose. We determine if several hours of controlled elevation of IOP (CEI) will produce the optic nerve head (ONH) gene expression changes and optic nerve (ON) damage pattern associated with early experimental glaucoma in rats.

Methods. The anterior chambers of anesthetized rats were cannulated and connected to a reservoir to elevate IOP. Physiologic parameters were monitored. Following CEI at various recovery times, ON cross-sections were graded for axonal injury. Anterior ONHs were collected at 0 hours to 10 days following CEI and RNA extracted for quantitative PCR measurement of selected messages. The functional impact of CEI was assessed by electroretinography (ERG).

Results. During CEI, mean arterial pressure (99 ± 6 mm Hg) and other physiologic parameters remained stable. An 8-hour CEI at 60 mm Hg produced significant focal axonal degeneration 10 days after exposure, with superior lesions in 83% of ON. Message analysis in CEI ONH demonstrated expression responses previously identified in minimally injured ONH following chronic IOP elevation, as well as their sequential patterns. Anesthesia with cannulation at 20 mm Hg did not alter these message levels. Electroretinographic A- and B-waves, following a significant reduction at 2 days after CEI, were fully recovered at 2 weeks, while peak scotopic threshold response (pSTR) remained mildly but significantly depressed.

Conclusions. A single CEI reproduces ONH message changes and patterns of ON injury previously observed with chronic IOP elevation. Controlled elevation of IOP can allow detailed determination of ONH cellular and functional responses to an injurious IOP insult and provide a platform for developing future therapeutic interventions.

Keywords: glaucoma, optic nerve head, intraocular pressure, animal models

Understanding the cellular mechanisms that underlie glaucomatous optic nerve damage is essential for developing new glaucoma therapies that can be used to augment established pressure-lowering treatments. This involves identifying the cellular events by which elevated IOP, a major risk factor for glaucoma, produces axonal injury and retinal ganglion cell (RGC) death. Because of the complexity of the optic nerve head (ONH), the likely site of axonal injury,[1–4] animal models should maintain the integrity of the ONH, including its blood supply and close interrelationship between axons, their supportive astrocytes, and surrounding connective tissues. Developing such models to mimic the characteristics of open angle glaucoma, with an emphasis on establishing a chronic, sustained elevation of IOP, has long been a major goal.[5–9]

Obstructing aqueous humor outflow in nonhuman primates using laser-induced scarring of the trabecular meshwork provides the most relevant paradigm to human glaucoma.[10] Such models have provided important information on IOP-induced physical forces within the ONH and how the presence of its abundant connective tissues, particularly the lamina cribrosa, may mediate and react to these forces. However, this work must necessarily be limited to small numbers of animals, making it less suitable for molecular biology studies. For this reason, experimental and genetically-induced outflow obstruction models in rodents have gained increasing popularity as glaucoma models.[5,9,11–17]

Over the past 20 years, work with several such models has yielded important information on the site of injury,[3,18] the mechanism of cellular death of RGCs,[19,20] and gene expression changes that accompany optic nerve damage from elevated IOP in the retina and optic nerve head.[21–25] However, interpreting these changes is challenging. If they are initial responses to the pressure stimulus, these could be either injurious (causing primary axonal injury) or protective. Alternatively, these responses could be late and secondary to axonal loss.

Making these determinations requires an understanding of the extent and duration of IOP elevation, which is a significant challenge with all chronic glaucoma models. Obstruction of aqueous humor outflow often results in marked fluctuations in

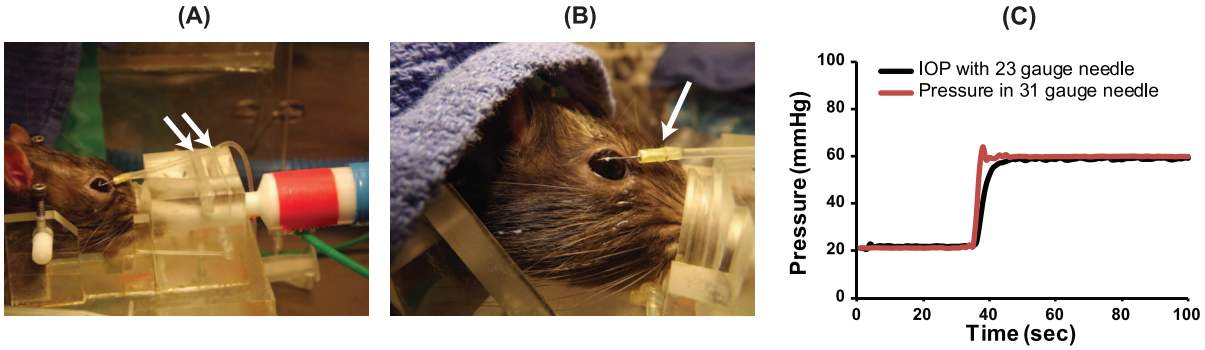

Figure 1. Controlled elevation of IOP. (**A**) Custom-made head holder, anchoring the nose in the respiratory cone, with isoflurane delivery (*green tube*) and an active exhaust for waste gas and CO_2 (*red* and *white fitting*). Balanced saline solution (BSS) tubing is anchored to the holder by two Silastic bands (*arrows*) that stabilize the needle, yet still allow delicate adjustment of the needle position in the eye. (**B**) Balanced salt solution PLUS delivered through the cornea using a modified, 31-gauge needle shortened to 1 cm with a modified bevel, the hub of which is fitted to flexible Silastic tubing (*single arrow*). Fixation of the animal's head and the tubing to the same holder minimizes chance of the needle becoming dislodged. (**C**) Intraocular pressure measured via a second anterior chamber needle (23-gauge) closely follows the intended pressure, delivered through a 31-gauge needle, when IOP is raised from 20 to 60 mm Hg, confirming that pressure measured in the 31-gauge needle line accurately reflects actual IOP.

IOP,[26–29] which can be missed by intermittent tonometry. At present, continuous telemetric pressure monitoring still is in its infancy,[30,31] although initial experience shows that fluctuations in IOP are likely to be and can be unexpectedly large.[32]

We have found, while studying chronic glaucoma in Brown Norway rats, that seemingly small IOP elevations can create focal optic nerve injury.[24,26,33] In addition, other investigators have shown that a few hours of IOP elevation are sufficient to produce reversible alterations in electroretinography (ERG)[11,34,35] and astrocyte morphology.[36] These observations suggest that the rodent ONH is relatively sensitive to IOP and that a short period of IOP elevation, in which IOP is controlled, may offer an opportunity to circumvent the limitations of chronic glaucoma models.

We demonstrated that several hours of exposure to a known level of elevated IOP (controlled elevation of IOP [CEI]) in Brown Norway rats can produce axonal injury and ONH gene expression changes that are similar to those described previously in an established, chronic IOP elevation model. We described this method and its effects on animal physiology, the anatomic and functional evidence of optic nerve injury, and initial observations of the resulting ONH gene expression changes.

Materials and Methods

Animals

Male Brown Norway rats, aged 6 to 8 months old ($n = 122$) were used in these experiments. Males were chosen to allow comparison of gene expression responses from this new model to our published results with chronic IOP elevation, which were based on male animals, whose docile nature allows reliable measurement of awake IOP.[12] All protocols conformed to the Association for Research in Vision and Ophthalmology Statement for the Use of Animals in Ophthalmic and Vision Research, and were approved by the Oregon Health and Science University Institutional Animal Care and Use Committee.

Anesthesia

Animals, routinely four at a time, were anesthetized by induction with 5% isoflurane (Piramal Healthcare, Mumbai, India), which then was reduced to 2% for the period of IOP exposure, using 100% O_2 as the carrier gas. Isoflurane was administered with a portable anesthesia machine (PAM) and OHIO Isoflurane vaporizer using a Multiplex Delivery System with 4 flowmeters and inline humidifiers. Animals were placed in custom-built holders that stabilized the head, allowing access to the eyes, incorporating a cone covering the external nares, leading to anesthesia (Fig. 1A). Waste anesthesia gas was actively collected with a Hallowell WAG interface valve connected to house vacuum for removal of excess gas and CO_2. The portable anesthesia machine and accessories were sourced from Patterson Scientific (Bend, OR, USA). Anesthetic delivery and waste gas removal were set up in parallel for all four animals, coming from or leading to a common unit.

CEI Exposure Paradigm

After topical 0.5% proparacaine application (Alcon Laboratories, Inc., Fort Worth, TX, USA), a sterile disposable 31-gauge needle, attached to Silastic tubing, was inserted obliquely (to produce a self-sealing wound) through the cornea into the anterior chamber. (Figs. 1A, 1B) To minimize lens and iris damage, the needle was shortened to 1 cm and resharpened to a 25° tri-bevel. The plastic hub was trimmed and connected to Silastic tubing (Catalog #508-004; inner diameter/outer diameter [ID/OD] = 0.7/1.65 mm; Dow Corning, Corning, NY, USA). Two elastic bands (Fig. 1A, arrows) stabilized the needle and also allowed accurate adjustment of the needle position.

Each Silastic tube was connected to larger tubing leading to a 4-way manifold connected to a single reservoir that could be raised or lowered to adjust inflow pressure, monitored by an in-line pressure transducer. The entire system was filled with BSS Plus (Alcon Laboratories, Inc.). Success at producing the desired IOP was confirmed in separate experiments using a transducer connected to a second anterior chamber cannula (23 gauge) to directly measure IOP (Fig. 1C).

All animals were wrapped in circulating warm water heating pads (38°C) and hydrated every 30 minutes with subcutaneous injection of 0.5 ml warm normal saline. Normal saline and topical 0.5% proparacaine were applied alternatively to both eyes every 15 minutes, and IOP was checked independently every 30 minutes with a TonoLab tonometer (Icare Finland Oy, Espoo, Finland) to detect deviations from the target pressure significant enough to warrant evaluating tube patency or leaks. At the end of CEI exposure, the IOP was reduced to normal and the needle carefully removed.

Erythromycin antibiotic ointment (0.5%) was applied to the experimental eye and the animals were kept warm and hydrated throughout recovery. All animals were killed under deep isoflurane anesthesia at different times following CEI exposure, depending on the specific experiment.

Because the extent and duration of IOP elevation can be controlled in this model, we have chosen to identify different combinations of these parameters by stating "CEI" followed by the IOP level and hours of exposure, so that elevation of IOP to 60 mm Hg for 8 hours is "CEI 60-8" and 20 mm Hg for 8 hours is "CEI 20-8".

Physiologic Monitoring

Physiologic monitoring was performed using a rat foot sensor connected to a MouseOxPlus Oximeter (STARR Life Sciences Corporation, Oakmont, PA, USA) with temperature and recording module, using an 8-channel multiplexer to allow monitoring of multiple animals. With this, real-time monitoring and recording of percent oxygen saturation of functional arterial hemoglobin, heart rate, respiratory rate, and pulse and respiratory distention could be performed, with rectal temperature in 1 of every 4 animals.

For blood pressure monitoring, animals were anesthetized with isoflurane, laid supine, and the tail artery cannulated with Tygon S-54-HL tubing, leading to a research grade blood pressure transducer (Harvard Apparatus, Holliston, MA, USA) with analog voltage output. The output of the pressure transducer was connected to a National Instruments Analog Input Module, with the signal recorded by National Instruments Signal Express Data Logging and Interactive Measurement Software (National Instruments, Austin, TX, USA). Mean blood pressure, with standard deviation, then was calculated for each animal from a decimated log of the pressure recording. In preliminary experiments, direct comparisons of tail artery pressures to readings from a similarly cannulated femoral artery produced identical readings between the 2 sites (data not shown).

In one group of 6 animals, all physiologic parameters, including blood pressure, were monitored continuously and recorded (1 Hz) for an entire 8 hours of anesthesia.

Optic Nerve Injury Assessment

Development of axonal injury was initially determined at several time points following CEI in myelinated optic nerve segments (postfixed in 4% paraformaldehyde and 5% glutaraldehyde) obtained at the time of ONH harvest for gene expression analysis (described below). Two additional groups of animals, used only for axonal injury assessment, underwent CEI exposure of 50 and 60 mm Hg, respectively, and were perfusion-fixed with an initial bolus of 100 ml buffered 4% paraformaldehyde followed by 1000 ml of buffered 5% glutaraldehyde. Eyes were enucleated and immersed in 5% buffered glutaraldehyde. All fixatives were used at 4°C.

Axonal injury was assessed in myelinated optic nerve cross-sections qualitatively by grading the extent of axonal injury, and quantitatively by counting degenerating axons. Fixed nerve segments 1 to 2 mm from the globe were embedded in plastic, sectioned, and stained with toluidine blue. For qualitative injury grading, masked slides of the entire optic nerve cross-section were assessed by light microscopy for degenerating axons by at least four observers, using a grading scale of nerve injury ranging from 1 (normal) to 5 (total degeneration).[26]

For degenerating axon counts, nerve cross-sections that together covered the entire nerve cross-section were digitally photographed under oil immersion (×100). Deidentified images were evaluated separately by three observers who marked degenerating axons (identified by condensed axoplasm, presence of myelin remnants, or swollen, empty-appearing axons) using Photoshop (Adobe Systems, San Jose, CA, USA). The files then were unmasked and layered in Photoshop and combined to create a montage of each optic nerve cross-section. Axons identified as degenerating by at least two observers were tallied for each nerve. Mean numbers of degenerating axons for each group with SEM were calculated and compared to counts for control eyes.

For statistical comparisons, the mean grade (or mean number of degenerating axons, if less than grade 2) for each group was calculated.

Electroretinography (ERG)

For ERG, animals were dark adapted overnight (>12 hours) and prepared for recordings under dim red illumination ($\lambda >$ 600 nm). Initial anesthesia was accomplished by intraperitoneal injection of ketamine (37.5 mg/kg; JHP Pharmaceuticals, Rochester, MI, USA), xylazine (7.5 mg/kg; RXV, Greeley, CO, USA), and acepromazine maleate (1.5 mg/kg; VET ONE, Boise, ID, USA) with a supplemental dose of ketamine (15 mg/kg) given after 1 hour. Pupil dilation and topical corneal anesthesia were achieved using 0.5% tropicamide and 0.5% proparacaine respectively (Alcon Laboratories). Body temperature was maintained using a USB rechargeable warmer placed beneath the animal. Paired, custom-made silver chloride electrodes were placed on both eyes, with the reference electrode situated circumferentially around the corneoscleral limbus and the active electrode located at the corneal apex, using 0.5% carmellose (Allergan, Parsippany, NJ, USA) as a coupling agent. A subdermal needle electrode (Technomed Europe, Maastricht, Netherlands) at the tail base served as the ground. Animals were dark adapted for a further 10 minutes following electrode placement before commencing the recording protocol.

Bilateral simultaneous ERGs were recorded using the UTAS Visual Electrodiagnostic Testing System with brief, white light stimuli delivered through a Bigshot Ganzfeld integrating sphere (LKC Technologies, Gaithersburg, MD, USA). Scotopic threshold responses were obtained for white flash (<5 ms duration) stimuli, intensities ranging from –6.7 to –3.9 log cd.s.m–2 in 0.2 log unit increments, by averaging 30 sweeps per intensity with an interstimulus interval of 2 seconds. Scotopic ERGs (from –3.6 to 2.2 log cd.s.m–2) were recorded by averaging 3 sweeps, with the interstimulus interval progressively increasing from 10 to 120 seconds to allow complete recovery of the B-wave. All recordings included a 10-ms prestimulus baseline with data collected up to 500 ms after stimulus delivery.

Raw data were extracted using EMWin Software (LKC Technologies) and exported into Excel (Microsoft, Redmond, WA, USA) in digital voltage-time format for post hoc analysis. Following source data verification, ERG response amplitudes were measured at strict time criteria after the flash stimulus. For responses to dimmer stimuli, a fixed criterion of 120 ms was chosen to correspond to the peak of the scotopic threshold response (pSTR). For scotopic responses to brighter flash stimuli, fixed criterion times of 70 and 6.5 ms were used to measure the amplitudes of the B-wave and A-wave, respectively.

Eight animals had bilateral ERG recordings at baseline (mean of two separate recordings), followed by unilateral exposure to 60 mm Hg for 8 hours (CEI 60-8). Electroretinographs then were repeated 2 days and 2 weeks after CEI exposure. Intensity response functions of ERG response amplitudes for experimental eyes were plotted at baseline, which was compared to similar plots at 2 days and 2 weeks following CEI IOP exposure.

Gene Expression Analysis

Animals used for gene expression analysis were decapitated under deep isoflurane anesthesia. Globes with attached, myelinated optic nerves were quickly removed and placed in ice cold PBS, and tissues were kept ice cold for the following steps. After removing the optic nerve segment for injury analysis, the globe was opened, and the anterior chamber, lens, and retina removed. The nerve and ONH were removed using a trephine and separated from any attached sclera. The nerve head was placed in a custom matrix, trimmed to 0.4 mm length to include the unmyelinated and transition regions, placed in a microfuge tube and immediately frozen by plunging the tube into dry ice pellets and then transferred to a –80°C freezer for storage before RNA extraction.

Total RNA was purified from ONHs using the PicoPure RNA Isolation Kit, according to the manufacturer's instructions, which includes DNAase treatment (Molecular Devices, Sunnyvale, CA, USA). RNA was quantitated using the Quant-iT RiboGreen assay (Invitrogen, Carlsbad, CA, USA). Relative quantification by quantitative real-time reverse transcription PCR (qPCR) was performed as described previously.[25] Briefly, 30 ng of total ONH mRNA from each sample, as well as from a pooled ONH RNA standard curve, was reverse transcribed and amplified by PCR, using glyceraldehyde phosphate dehydrogenase (GAPDH) for normalization. Product identities were confirmed by sequencing. Primers were designed using Clone Manager (Sci-ed Software, State Line, PA, USA) using sequences for rat mRNAs available in the NIH National Center for Biotechnology Information databases. Quantitative real-time reverse transcription PCR was performed on messages obtained from ONH, providing enough material to test approximately 15 messages per ONH.

Effects of CEI on gene expression were determined in two experiments. In the first (CEI message experiment 1), 32 animals underwent CEI 60-8 and were killed either immediately (Time 0, without recovery from anesthesia) or at 12 hours, 3 days or 10 days after exposure ($n \geq 8$ per time point) and ONH gene expression compared to fellow eye controls at each time point. Messages explored encompassed interleukin 6-type cytokine signaling pathways, cell proliferation, specific cell markers, and extracellular matrix modifiers shown to be significantly regulated in our chronic model.[24,25] Controlled elevation of IOP message experiment 2 was designed to determine the effects of IOP, anesthesia, and anterior chamber cannulation on ONH gene expression. A total of 16 animals underwent CEI 60-8 and another 16 were exposed to 20 mm Hg for 8 hours (CEI 20-8). Half of each group was killed either immediately (Time 0) or 3 days after CEI exposure and compared to a group of naïve animals (anesthesia only before sacrifice and no anterior chamber cannulation). Messages evaluated were similar, but not identical, to those used in CEI message experiment 1. Messages selected for evaluation, including official and alternative gene names and official gene acronyms, are listed in Table 1. Primers used are listed in Supplementary Table S1.

Statistical Analysis

Group means (± SD for physiologic parameters and TonoLab IOP measurements; ± SEM for nerve injury) were calculated and comparisons were performed by *t*-test or ANOVA using Graphpad Prism software (La Jolla, CA, USA). For ERG analysis, statistical comparison for each of the three respective responses was performed with a 2-way ANOVA with repeated measures using Graphpad Prism software, with a null hypothesis that no differences exist between the intensity-response relationships recorded at baseline and those recorded after IOP elevation. This analysis aimed to compare the intensity-response relationships as a whole, rather than to test differences at individual intensities, which are otherwise generally correlated within each eye. For gene expression analysis, the significance of differences between groups for each studied message was determined by 1- or 2-way ANOVA with Dunnett's post test (or the Kurskal-Wallis test with Dunn's post test if Bartlett's test for equal variances on the data without or with log2 transformation indicated a significant difference between the variances).

Table 1. Messages Evaluated: Official Gene Names and Acronyms

Official Gene Name (Alternative Name)	Gene Acronym
Allograft inflammatory factor 1 (Iba1)	*Aif1*
Aquaporin 4	*Aqp4*
Cd68 molecule	*Cd68*
Fibulin 2	*Fbln2*
Growth associated protein 43	*Gap43*
Glyceraldehyde phosphate dehydrogenase	*Gapdh*
Glial fibrillary acidic protein	*Gfap*
Gap junction protein alpha 1 (Connexin 43,Cx43)	*Gja1*
Interleukin 6	*Il6*
Integrin subunit alpha V	*Itgav*
Leukemia inhibitory factor	*Lif*
Leukemia inhibitory factor receptor	*Lifr*
Neurofilament, light polypeptide	*Nefl*
Purinergic receptor P2Y12	*P2ry12*
Periostin (Osf2)	*Postn*
Protein regulator of cytokinesis 1	*Prc1*
Rho associated coiled-coil containing protein kinase 2	*Rock2*
Suppressor of cytokine signaling 3	*Socs3*
Transforming growth factor beta 2	*Tgfb2*
Tenascin c (Hxb)	*Tnc*
Topoisomerase (DNA) II alpha	*Top2a*

Results

Animal Physiology Under Isoflurane Anesthesia

To determine the stability of physiologic parameters over a typical CEI exposure, 6 animals were continuously monitored for 8 hours under 2% isoflurane and the conditions described in Methods. Mean systemic blood pressure for this group was 99 ± 5 (SD) mm Hg while mean oxygen saturation, heart rate, and respiratory rate were 99.2 ± 0.2%, 338 ± 11 beats per minute, and 56 ± 12 breaths per minute, respectively. Figure 2 shows a continuous tracing of these parameters in one animal, demonstrating stability over the entire 8 hours. Table 2 presents two values for each parameter, each representing a mean of all 6 animals, over two 15-minute periods, one beginning 30 minutes after the onset of anesthesia and the other ending 30 minutes before the end of anesthesia. There were no significant differences between the beginning and ending means for any of these parameters.

Overall, in 34 animals under anesthesia, isolated measurements of systemic blood pressure ranged from 89 to 121 mm Hg, with a mean of 99 ± 6 (SD) mm Hg. In 18 animals undergoing CEI, mean oxygen saturation, heart rate, and respirations over the entire 8 hours were determined for each animal and these then were used to calculate a group mean for each parameter. These resulting overall means were 99.1 ± 0.3% (range, 99–100%), 294 ± 25 beats per minute (range, 254–343), and 48 ± 10 breaths per minute (range, 36–76), respectively.

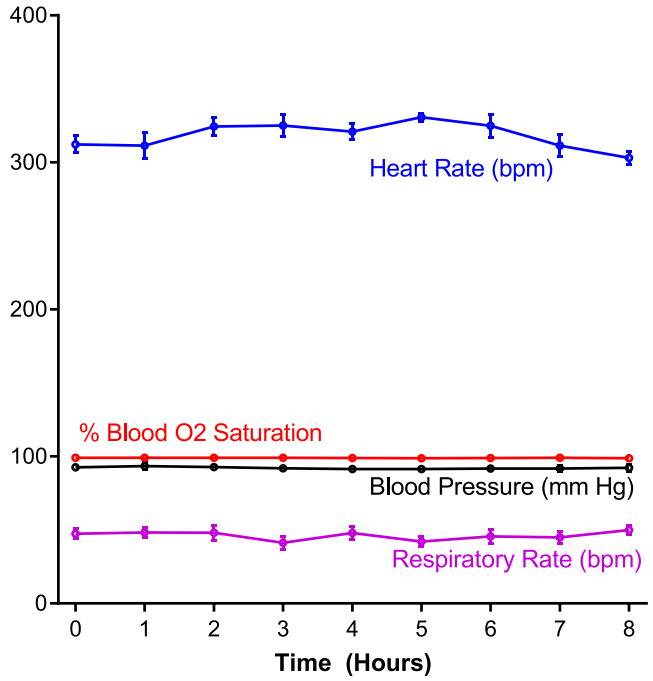

Figure 2. Continuous tracing of heart rate, percent blood oxygen saturation, systemic blood pressure, and respiratory rate over 8 hours in one animal under 2% isoflurane anesthesia. Note stable values for all parameters over the entire observation period. *Error bars*: standard deviation.

TonoLab IOP

In 45 eyes exposed to CEI 60-8, mean TonoLab readings for the experimental eyes was 57 ± 3 mm Hg (mean ± SD), while that of uncannulated, fellow eyes was 9.0 ± 1 mm Hg. This was confirmed by observations from CEI message experiment 2, shown in Table 3. This Table summarizes IOPs in 32 additional animals, 16 of whom underwent CEI 60-8 while the other 16 were exposed to CEI 20-8. TonoLab readings (mean ± SD) confirmed that IOP targets were achieved for both experimental eye groups (CEI 60-8 = 57 ± 2 mm Hg and CEI 20-8 = 22 ± 2 mm Hg). Mean TonoLab readings for all control fellow eyes in this experiment ($n = 32$), under anesthesia, was 8 ± 1 mm Hg. All fellow eye pressures were well below that of previously reported awake TonoLab IOP readings for normal eyes,[37] which is most likely due to the pressure-lowering effects of isoflurane anesthesia.[38]

Axonal Injury

Postfixed optic nerves revealed that optic nerve injury grade was not significantly increased until 10 days following CEI exposure (Fig. 3A) In 8 additional animals, perfusion-fixed for assessing axonal degeneration, the injury grade 10 days after CEI was 2.02 ± 0.26 (SEM) versus 1.03 ± 0.01 in fellow controls ($P < 0.002$). This group demonstrated a mean (± SEM) degenerating axon count of 321 ± 107 per nerve compared to 16 ± 4 for fellows ($P < 0.002$; Figs. 3B, 3C). In another group of 8 animals, exposed to 50 mm Hg for 8 hours (CEI 50-8), mean degenerating axons per nerve was 42 ± 11, also significantly greater than that of fellow controls ($P < 0.03$). From these groups, along with additional CEI 60-8 animals, a total of 23 nerves with early injury was found in which the ophthalmic artery was present, which lies inferior to the optic nerve and provides a landmark for orientation.[39] Of these, 19 (83%) demonstrated a focal injury located in the superior region of the optic nerve (Figs. 3D, 3E).

Table 2. Physiologic Parameters for 6 Animals Over an 8-Hour Period, Comparing Means of a 15-Minute Period 30 Minutes After the Beginning of Anesthesia to a Similar Period 30 Minutes Before the End

Physiologic Parameter	Beginning ± SD	Ending ± SD	*P* Value*
Blood pressure, mm Hg	96.7 ± 3.7	98.1 ± 3.6	0.26
% Blood O_2 saturation	99.3 ± 0.2	99.3 ± 0.1	0.53
Heart rate, bpm	346 ± 13	323 ± 30	0.13
Respiratory rate, bpm	53 ± 16.3	50 ± 11.3	0.28

* Differences between the beginning and ending values were not statistically significant (paired *t*-test).

Table 3. TonoLab IOP Readings for Animals Exposed for 8 Hours to Either 60 mm Hg (CEI 60-8) or 20 mm Hg (CEI 20-8) Compared to Fellow, Uncannulated Eyes

Cei Condition	60-8	20-8	All Fellow Eyes
Mean IOP ± SD, mm Hg*	57.2 ± 2.2	22.1 ± 2.3	8.3 ± 1.1
n	16	16	32

* A total of 16 measurements were made per animal.

Electroretinography

Intensity response curves for pSTR, B-wave, and A-wave amplitudes at 2 and 14 days following IOP exposure compared to baseline levels are shown in Figure 4. Significant, transient reductions in pSTR (51.9 ± 12.4%; $P < 0.0001$), B-wave (19.5 ± 9.8%; $P < 0.0001$), and A-wave (67.2 ± 4.8%; $P < 0.0001$) responses were observed 2 days following the CEI exposure. Two weeks after IOP exposure, no lasting impact upon the B-wave or A-wave responses (representing bipolar cell and photoreceptor function, respectively) was observed, with amplitudes comparable to baseline levels ($P > 0.05$). However, a small, but significant, residual deficit in the pSTR response (representing RGC function) was evident at this time point ($P = 0.005$).

ONH Gene Expression Changes in Response to CEI 60-8 (CEI Message Experiment 1)

We initially asked if selected gene expression responses previously determined to occur in studies of our chronic glaucoma model also would be observed following CEI[24,25] (See Table 1 for full gene names and acronyms). Because we knew the onset and duration of CEI exposure, we also were able to determine, by euthanizing animals at specific time points, the relative timing of these different responses, as well as their recovery patterns. These results are summarized graphically in Figure 5. Specific values for all of these messages at each time point are listed in Supplementary Table S2.

Immediately following CEI (Time 0, without any recovery from anesthesia) the most profoundly regulated messages were consistent with interleukin 6-type cytokine signaling (Fig. 5A). Cytokines *Il6* and *Lif* demonstrated an immediate, significant elevation. Whereas *Il6* normalized by 3 days, *Lif* remained significantly elevated, even at 10 days, albeit substantially reduced from its earlier peak. *Socs3*, a negative feedback regulator of Jak-Stat signaling, also was significantly elevated at Time 0. This normalized by 10 days, although not as rapidly as *Il6*. *Lifr* expression, the protein of which can be reduced in astrocytes by *Lif*,[40] exhibited a significant reduction, apparent

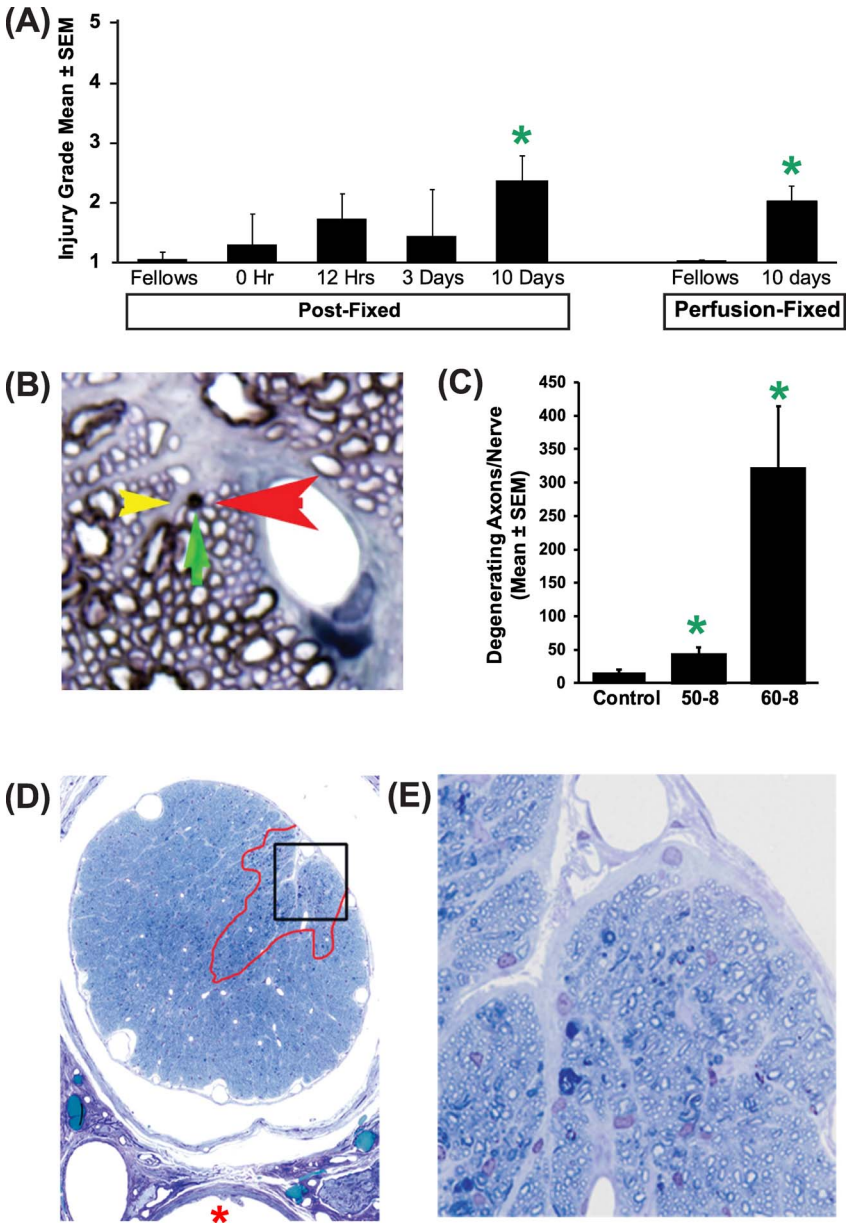

Figure 3. Optic nerve injury following CEI. (**A**) Assessment of axonal injury grade in postfixed optic nerve cross-sections shows that significant injury does not appear until 10 days following CEI exposure. Two columns on *far right* demonstrate injury grade in perfusion-fixed experimental and control eyes 10 days after CEI 60-8 (n = a minimum of 8 for all groups). (**B**) Degenerating axon identified by 3 observers (*arrows*) under oil immersion for degenerating axon counts. (**C**) Degenerating axon counts are significantly higher in CEI 60-8 and CEI 50-8 nerves than in fellow control eyes. (**D**) Cross-section of CEI 60-8 nerve (injury grade 2.14), showing superior location of injury (*red outline*) relative to inferiorly located ophthalmic artery (*red asterisk*). (**E**) Detail of degenerating axons in boxed area from (**D**). Asterisks in (**A**) and (**C**) indicate a statistically significant difference from control values ($P < 0.05$).

at Time 0, with no evidence of recovery over the entire follow-up period.

Markers for cell proliferation, *Top2a* and *Prc1*, also demonstrated significant increases in gene expression. However, this was delayed. After an initial, nonsignificant depression, messages for both markers were significantly elevated at 3 days and remained so at 10 days, with some evidence of recovery. *Tgfb2*, hypothesized to promote fibrotic changes in the glaucomatous optic nerve head,[41–43] was significantly reduced by 12 hours after exposure and remained so through the remainder of the 10-day postexposure observation period. This was consistent with our chronic model observations,[24] *Postn*, *Tnc*, and *Fbn2*, representing the matricellular class of extracellular matrix proteins, were all significantly elevated at 12 hours and 3 days, with signs of normalization by 10 days.

Figure 5B illustrates message responses for cell-type markers. The axonally-contained mRNA *Nefl* polypeptide and *Gap43* were initially increased. However, both demonstrated a significant decrease 3 days after IOP exposure which, by 10 days, was further reduced to as little as 16% and 27% of control values, respectively.

Astrocyte markers *Gfap*, *Gja1* (or Connexin 43), and *Aqp4* all failed to demonstrate significant elevations. Rather, *Gja1* was significantly reduced immediately after IOP exposure, and messages for all three were moderately, but significantly

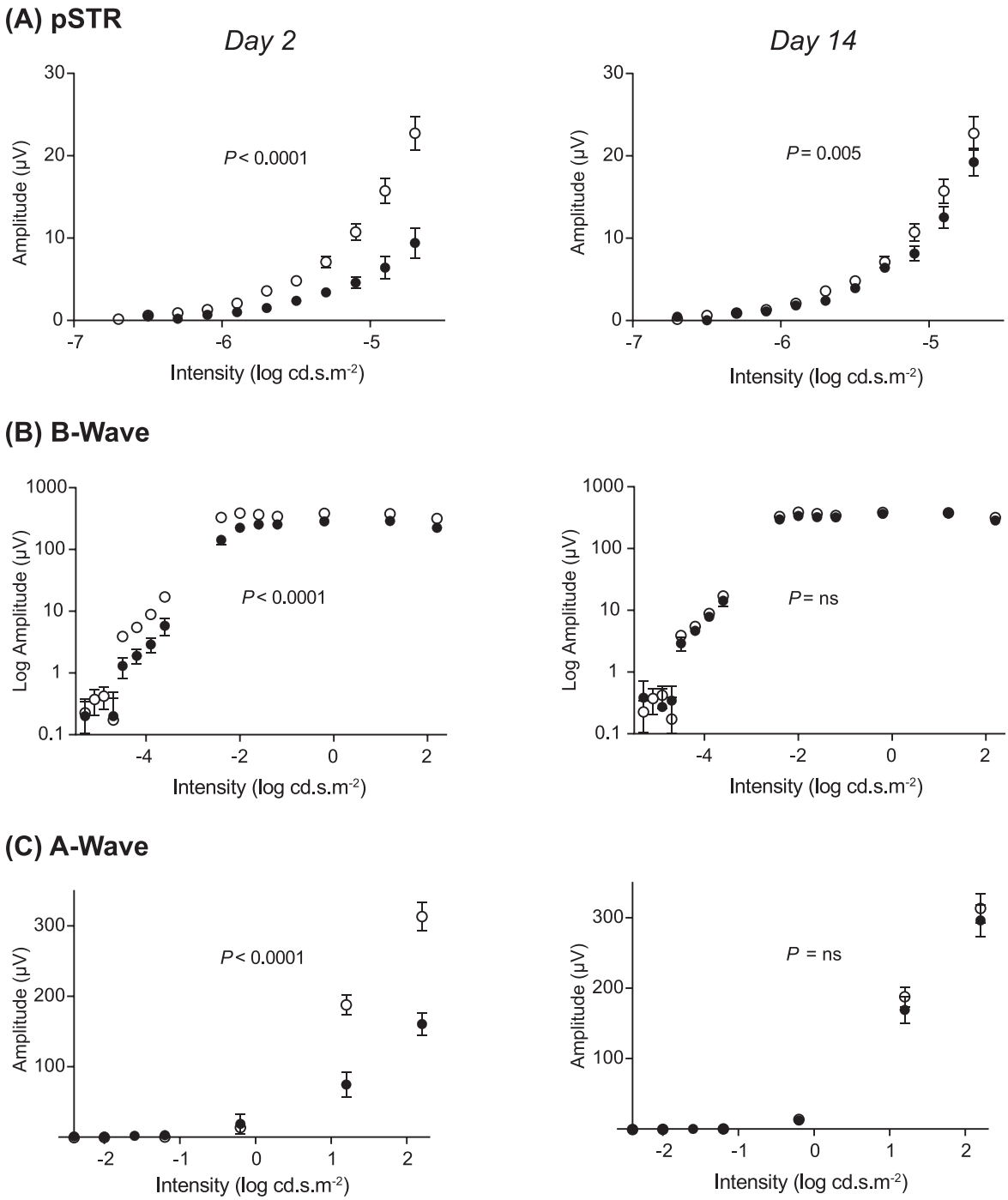

FIGURE 4. Intensity-response functions of eyes 2 days (*left panel*) and 14 days (*right panel*) following CEI 60-8 exposure compared to baseline. Electroretinogram amplitude (group mean ± SEM) versus stimulus intensity for eyes following CEI (*filled symbols*, $n = 8$) and baseline (*open symbols*, $n = 8$). (**A**) Positive scotopic threshold response (pSTR) amplitude measured at 120 ms after the stimulus flash. (**B**) Scotopic B-wave amplitude measured at 70 ms after the stimulus flash. (**C**) Scotopic A-wave amplitude measured at 6.5 ms after the stimulus flash.

reduced 12 hours after IOP elevation. All returned to normal by day 3.

The microglial marker *P2ry12*, abundant in brain microglia,[44] was significantly decreased initially but normalized by day 3. Such decreases may be associated with microglial process retraction to a more ameboid (activated) morphology.[45] *Aif1* (or *Iba1*) demonstrated a small, but significant increase at day 3.

ONH Message Changes Are Not Associated With Cannulation or Prolonged Anesthesia (CEI Message Experiment 2)

Here, animals were exposed unilaterally to either CEI 60-8 or CEI 20-8 and killed at either Time 0 or 3 days after IOP exposure. Message responses for all groups of ONHs were compared to a separate group of ONH from naïve eyes that had undergone neither prolonged anesthesia nor cannulation.

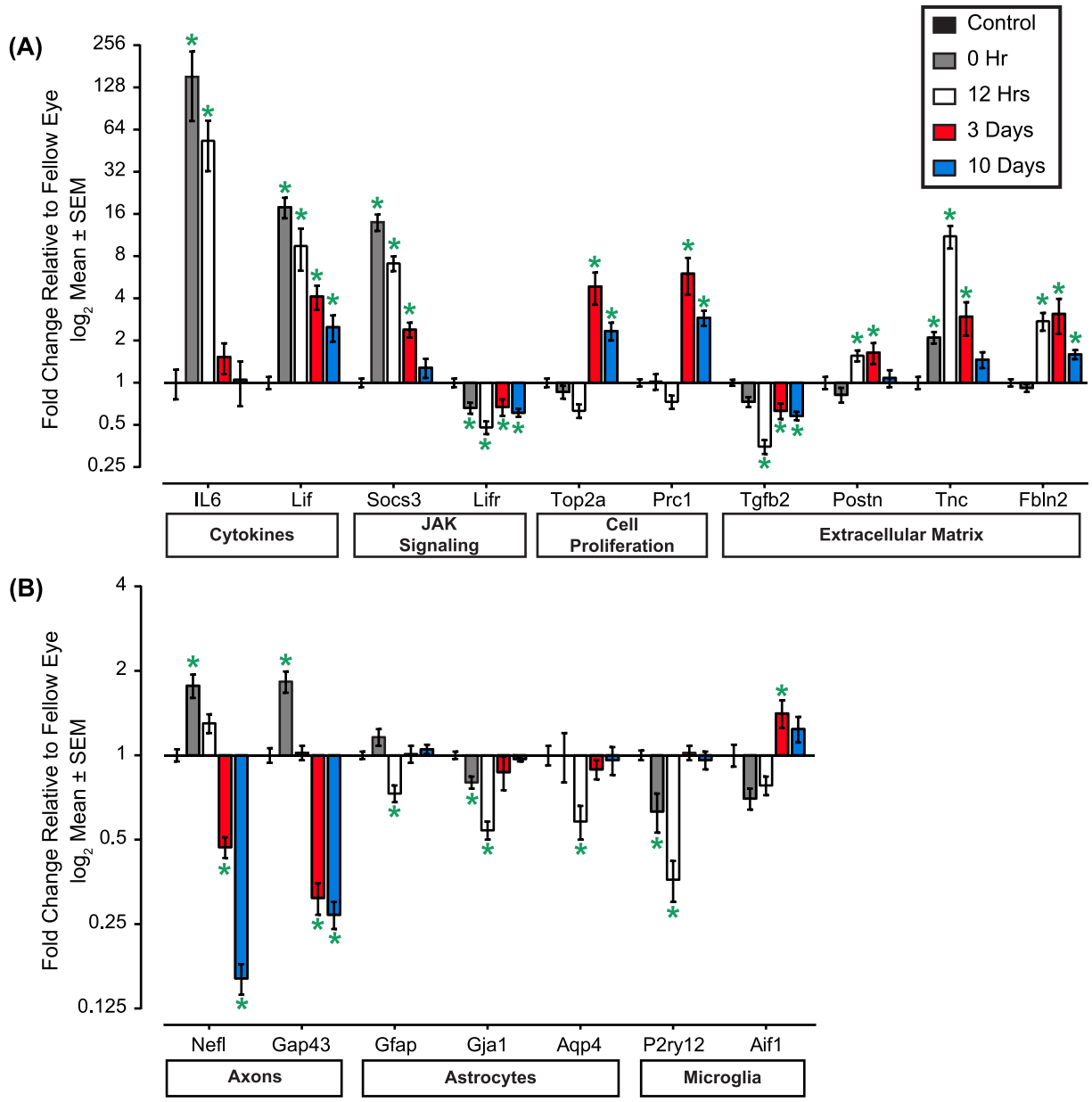

Figure 5. Initial observations on message responses, compared to control eyes, immediately after IOP exposure (0 hours), along with recovery times of 12 hours, 3 days, and 10 days. (**A**) IL6-type and JAK signaling demonstrate robust, early response while significant gene expression changes associated with cell proliferation are delayed to day 3. Message levels for the cytokine *Tgfb2* are downregulated during recovery. Matricellular proteins *Tnc*, *Postn*, and *Fbln2*, show patterns of upregulation that peak between 12 hours and 3 days after CEI exposure. (**B**) Cell-type markers show various response patterns. Axonal-associated mRNAs are initially elevated at 0 time, and dramatically fall during recovery. Astrocyte markers are transiently depressed at 3 days, but then recover. Microglial *P2ry12* demonstrates a transient but significant downregulation, followed by normalization. *Aif1* levels are significantly increased at 3 days recovery. Note that the *y*-axis is a log2 scale that is different in magnitude between the two charts. *Indicates a statistically significant difference from control values. *n* is equal to or greater than 8 per group. For each message, control eye variability is indicated by the *error bars* on the *left*.

Significant differences were seen only in ONHs undergoing CEI 60-8 and these appear in Table 4. Neither CEI 20-8 nor fellow control ONHs of either experimental group (anesthesia only) demonstrated significant message level responses compared to naïve tissues. All responses, compared to naïve ONHs, are listed in Supplementary Table S3.

Among messages not evaluated in CEI message experiment 1, *Rock2*, important for modulating actin cytoskeleton organization and cell adhesion, was mildly, yet significantly elevated 3 days following CEI-60. Cell markers for astrocytes (*Gfap*), microglia (*Cd68*), and the vascular-associated *Itgav* all failed to show significant changes in any condition and at any time point.

Discussion

Working with an established model of chronic IOP elevation, we have reported previously that mild or early optic nerve damage is associated with prominent changes in ONH gene expression for processes involved in interleukin 6-type cytokine signaling and cell proliferation, as well as alterations

Table 4. Significant Gene Expression Responses Following 8 Hours' Exposure to 60 mm Hg (CEI 60-8) Versus 20 mm Hg (CEI 20-8), to Determine the Effect of Anesthesia, Anterior Chamber Cannulation and Elevated IOP

	CEI 60-8 Recovery Time		CEI 20-8 Recovery Time	
Message	**0 Time**	**3 Days**	**0 Time**	**3 Days**
Il6	11,064% ± 4391%*	123% ± 29%	200% ± 58%	114% ± 66%
Lif	8520% ± 3200%*	793% ± 335%	124% ± 20%	116% ± 20%
Nefl	143% ± 27%	54% ± 7%*	184% ± 41%	89% ± 24%
Rock2	133% ± 11%	137% ± 11%*	110% ± 13%	112% ± 10%
Tgfb2	79% ± 11%	69% ± 6%*	81% ± 4%	110% ± 7%
Top2a	79% ± 14%	279% ± 86%*	90% ± 11%	106% ± 16%

* Indicates significant change compared to Naïve ONH. Only CEI 60-8 ONH demonstrated significant changes in gene expression compared to naïve ONH. Five other messages (*Cd68*, *Gfap*, *Intga*, *Postn*, and *Tnc*) were not significantly changed in expression in this study. Complete results, including message values in anesthetized fellow eyes are available in Supplementary Table S3. $n \geq 7$ for all groups.

in the extracellular matrix and several cell-type markers.[24] However, while IOP can be measured at frequent intervals, the exact level and duration of pressure elevation still cannot be determined without continuous telemetric IOP monitoring. As a result, the precise timing and relationships of these responses to each other, and to the injury itself, is unknown; some could be initial, injury-initiating responses, while others may be secondary to axonal injury, or protective reactions. To address this problem, we decided to determine if axonal injury and ONH gene expression changes known to occur in chronic glaucoma models[24,25] also would be observed using controlled elevation of IOP applied over a time period suitable for laboratory study.

Initial experiments using IOPs of 40 mm Hg and 4-hour exposures led to moderate gene expression changes but inconsistent evidence of optic nerve injury (data not shown). We ultimately decided to use an 8-hour pressure exposure, as this offered a better opportunity to produce focal axonal injury and significant ONH responses. Abbott et al.[46] have reported that an 8-hour exposure to 50 mm Hg in rats produced initial nerve fiber layer thickening as determined by spectral domain optical coherence tomography, but no significant long-term thinning, RGC loss or lasting deficits in axonal transport.[46] By assessing axonal injury,[26,47] we found in our present CEI model that 50 mm Hg produced axonal injury that could be detected only by quantifying degenerating axons (Fig. 3C). By comparison, 60 mm Hg produced optic nerve injury identifiable by qualitative and quantitative methods. This pressure is equal to peak IOPs reported in chronic models using nonhuman primates[27,28,48] and rodents,[14,49–52] yet still is well below the 110 to 120 mm Hg generally used for studying ischemia/reperfusion.[53,54] Although degenerating axon counts, performed by light microscopy are likely an underestimate of total injury, the extent of axon loss in this model is mild and likely less than inter-eye variability in axon count.[55]

An essential feature of the CEI model is the high degree of control it provides over the extent and duration of IOP exposure. As shown in Figure 1C, actual IOP closely mirrors the intended pressure. The extensive TonoLab data in Table 2, consisting of 16 readings per animal over the entire 8 hours, further supported this, and demonstrated that pressures can be efficiently and uniformly delivered to as many as 4 animals at a time.

Because the CEI model requires IOP elevation for several hours, general anesthesia is essential. We chose to use inhalational isoflurane as it produces excellent general anesthesia with minimal animal movement which, coupled with flexible tubing and specific features of the head holder, successfully minimized intraocular trauma. Because this agent can lower systemic blood pressure, we carefully monitored this parameter and found that, using the conditions described here, including active removal of waste gas and CO_2,[56] mean blood pressure averaged 100 mm Hg. This is comparable to that reported in rats using isoflurane for shorter periods of time, as well as other anesthetics.[57–59] Importantly, through continuous monitoring, we confirmed that blood pressure, as well as heart rate, oxygen saturation, and respiratory rate, all remained stable over the entire 8 hours.

Given this level of systemic blood pressure, an IOP of 60 mm Hg provides a perfusion pressure of 40 mm Hg, which is sufficient to maintain retinal and ONH perfusion to at least 80% of baseline, as determined previously using optical coherence tomography angiography[56,60,61] and other methods.[62] Above 60 mm Hg, perfusion decreases rapidly. Bui et al.[35] showed that an IOP of 60 mm Hg or less for 105 minutes allowed full recovery of all components of the ERG, whereas 70 mm Hg or higher prevented full recovery of the ERG and produced cell loss in the RGC layer. They concluded that there exists a "threshold" between 60 and 70 mm Hg, above which permanent functional retinal loss will occur, most likely due to ischemia.[35,63]

Our electrophysiologic findings confirmed these results. They also showed that extending exposure at 60 mm Hg to 8 hours, well beyond the 105 minutes reported by Bui et al.,[35] does not have a lasting effect upon major components of either the outer or inner retinal function, represented by the A-wave and B-wave intensity plots, respectively. Both were unaffected 2 weeks following this single insult, confirming the absence of long-term ischemic sequelae.

However, our 2-week data did reveal a small, but statistically significant residual reduction in the pSTR. This component of the ERG has been shown to correlate well with damage to RGC soma in the inner retina and axons within the optic nerve[64,65] and this finding is consistent with our histologic observation of mild axonal injury within the optic nerve (Fig. 3). Thus, it appears that extending exposure to 8 hours elicits a selective effect on the pSTR. Since this component of the ERG has been associated with injury from lower levels of IOP elevation in our chronic model,[49] this supports the applicability of ONH findings in the CEI model to chronic animal glaucoma models, as well as to human glaucoma.

It is important that optic nerve injury in this model is primarily focal and located in the superior region of the optic nerve. This is consistent with superior peripapillary retinal thinning observed by Fortune et al.[66] during acute IOP elevation in rats and with observations in chronic models by ourselves[5] and several other investigators. Dai,[67] using intracamerally injected magnetic microspheres to elevate IOP, described ultrastructural evidence of axonal degeneration in the superior ONH and proposed a mechanism for this based on changes in astrocyte morphology in this region. Others, using laser-induced IOP elevation, reported preferential loss of nerve fiber layer axons and RGCs in the superior retina in rats[29,68,69]

and mice.[70] Recently, Pazos et al.[71] have noted that axon bundles in the superior region of the rat ONH are closely associated with Bruch's membrane, whereas inferior bundles are separated from Bruch's by the central retinal vein and artery.[71] Since this connection may allow more direct transmission of mechanical stress from elevated IOP to the superior neural tissue, this could provide an anatomic explanation for regional susceptibility in these models. Further work with the CEI model will help reveal the cellular basis for this phenomenon and provide new insights into axon injury mechanisms associated with elevated IOP.

While future work will carefully assess genome-wide expression in the optic nerve head tissue in this model, the qRTPCR data from CEI message experiments 1 and 2 do demonstrate that the CEI approach can produce many of the gene expression changes that already have been observed in the hypertonic saline chronic model, summarized in Supplementary Table S4.[24] All of these occurred only in eyes with elevated IOP, confirming that these responses are associated with elevated IOP and not the result of either anesthesia or anterior chamber cannulation. It is important to note that this association is not proof that these responses all contribute to chronic injury. While they might be integral to the fundamental molecular mechanism that leads to axonal injury and glaucomatous vision loss, they also could be secondary to axonal loss regardless of the primary insult, or they could be simply ONH cell responses to elevated IOP. Fortunately, the CEI model, with its tight control over IOP exposure, offers opportunities to differentiate among these possibilities.

In early glaucoma damage,[24] we noted that interleukin 6-type cytokine signaling processes were highly upregulated. These include *Il6* and *Lif*, which activate via the Jak-Stat pathway, leading to upregulation of the feedback inhibitor, *Socs3*, which also was elevated. This signaling pathway triggers cellular responses, including inflammatory, immune, and neuroprotective responses, as well as cell proliferation.[72] Because of the ability of this pathway to stimulate glial cell differentiation and proliferation,[24,73–76] we speculated then that interleukin 6-type cytokine alterations may be contributing to the proliferative responses we observed with early injury, demonstrated by upregulation of cell cycle genes *Top2a* and *Prc1* in the ONH.

In the CEI model, *Il6*, *Lif*, and *Socs3* were significantly upregulated immediately at Time 0 (Fig. 5A). By studying changes at progressively longer times following IOP exposure, we also were able to show that these changes preceded activation of cell proliferation, which was not evident until day 3. This chronology, something that we could not demonstrate with our chronic model, is consistent with the possibility that proliferation responses may, indeed, be driven, in part, by cytokine signaling.

In our assessment of cell markers, (Fig. 5B) we noted an initial increase in axonally-associated *Nefl* and *Gap43*, which may represent obstruction of axonal transport during IOP elevation. Interestingly, this was followed by a significant reduction that continued to decrease over 10 days to levels as little as 16% and 27% of baseline, respectively. This, too, is similar to what we observed previously in our chronic model.[24] While this could suggest profound axonal damage and potentially ongoing loss of RGCs, this seems unlikely as we have noted little evidence of increased injury at 14 and 21 days following CEI in subsequent experiments (data not shown). Regardless, these observations do suggest that IOP-induced abnormalities of axonal transport may be more complicated than currently appreciated and warrant further investigation in future studies using this model, including recovery times beyond the 10 days shown here.

Although developed to improve our understanding of early genomic responses of the ONH to elevated IOP, the CEI model offers opportunities to study other aspects of optic nerve as well as retinal damage. These include the role of preconditioning and prosurvival pathways in response to IOP, and the highly clinically relevant question of whether a repeat IOP exposure has a protective effect or actually leads to increased vulnerability of the nerve. The persistent depression of *Lifr*, despite recovery of its negative regulators *Lif* and *Socs3*,[40,77] present the possibility that complex delayed or altered recovery of certain responses may have an important role in the effect of repeat exposure on susceptibility. Additional uses could be to compare cellular mechanisms of axonal injury from IOP to those that result from other types of insults, including ischemia, direct axonal injury (experimental axotomy), and the influence of age on all of these processes. It should, however, be remembered that isoflurane does have neuroprotective properties.[78–80] While this does not appear to fundamentally affect the IOP-induced gene expression changes within the ONH, careful controls, similar to those used here, still must be employed, particularly if this model were to be used for experimental neuroprotection studies.

In summary, we have shown that a single, 8-hour CEI exposure reproduces significant, but mild optic nerve damage and gene expression changes within the ONH previously found to occur in chronic IOP elevation models. These responses are independent of anesthesia and anterior chamber cannulation. The stability of the IOP and its fidelity to the intended pressure, along with the stability of animal physiology over the entire experiment all support this as a reliable approach for studying ONH cellular processes involved in pressure-induced axonal injury.

Acknowledgments

The authors thank Phoebe Lin, MD, PhD, for generously providing access to instrumentation for electrophysiologic measurements.

Supported by National Institutes of Health (NIH; Bethesda, MD, USA) Grants NEI:R01EY-010145 and R01EY-016866 (JCM and ECJ), R01-EY019327 (BF), K08EY024025 (ST), and P30 EY010572 (OHSU); The US-UK Fulbright Commission in conjunction with Fight for Sight (HJ); The Special Trustees of Moorfields Eye Hospital (through an NIH Research award to Moorfields Eye Hospital NHS Foundation Trust and the UCL Institute of Ophthalmology for a Biomedical Research Centre for Ophthalmology) (HJ); American Glaucoma Society Young Clinician Scientist Award (ST); Glaucoma Research Foundation Shaffer Grant (ST); an unrestricted grant to OHSU from Research to Prevent Blindness (RPB), and an RPB Career Development Award (ST); and Legacy Good Samaritan Foundation (BF).

Disclosure: **J.C. Morrison**, None; **W.O. Cepurna**, None; **S. Tehrani**, None; **T.E. Choe**, None; **H. Jayaram**, None; **D.C. Lozano**, None; **B. Fortune**, Inotek, Inc. (C); **E.C. Johnson**, None

References

1. Quigley HA, Addicks EM. Regional differences in the structure of the lamina cribrosa and their relation to glaucomatous optic nerve damage. *Arch Ophthalmol*. 1981;99:137–143.
2. Quigley HA, Addicks EM, Green WR, Maumenee AE. Optic nerve damage in human glaucoma. II. The site of injury and susceptibility to damage. *Arch Ophthalmol*. 1981;99:635–649.
3. Schlamp CL, Li Y, Dietz JA, Janssen KT, Nickells RW. Progressive ganglion cell loss and optic nerve degeneration in DBA/2J mice is variable and asymmetric. *BMC Neurosci*. 2006;7:66.
4. Howell GR, Libby RT, Jakobs TC, et al. Axons of retinal ganglion cells are insulted in the optic nerve early in DBA/2J glaucoma. *J Cell Biol*. 2007;179:1523–1537.

5. Morrison JC, Moore CG, Deppmeier LM, Gold BG, Meshul CK, Johnson EC. A rat model of chronic pressure-induced optic nerve damage. *Exp Eye Res*. 1997;64:85–96.
6. Epstein DL, Freddo TF, Anderson PJ, Patterson MM, Bassett-Chu S. Experimental obstruction to aqueous outflow by pigment particles in living monkeys. *Invest Ophthalmol Vis Sci*. 1986;27:387–395.
7. Gaasterland D, Kupfer C. Experimental glaucoma in the rhesus monkey. *Invest Ophthalmol*. 1974;13:455–457.
8. Quigley HA, Addicks EM. Chronic experimental glaucoma in primates. I. Production of elevated intraocular pressure by anterior chamber injection of autologous ghost red blood cells. *Invest Ophthalmol Vis Sci*. 1980;19:126–136.
9. Pang IH, Clark AF. Rodent models for glaucoma retinopathy and optic neuropathy. *J Glaucoma*. 2007;16:483–505.
10. Burgoyne CF. The non-human primate experimental glaucoma model. *Exp Eye Res*. 2015;141:57–73.
11. Crowston JG, Kong YX, Trounce IA, et al. An acute intraocular pressure challenge to assess retinal ganglion cell injury and recovery in the mouse. *Exp Eye Res*. 2015;141:3–8.
12. Morrison JC, Cepurna WO, Johnson EC. Modeling glaucoma in rats by sclerosing aqueous outflow pathways to elevate intraocular pressure. *Exp Eye Res*. 2015;141:23–32.
13. John SW, Smith RS, Savinova OV, et al. Essential iris atrophy, pigment dispersion and glaucoma in DBA/2J mice. *Invest Ophthalmol Vis Sci*. 1998;39:951–962.
14. Samsel PA, Kisiswa L, Erichsen JT, Cross SD, Morgan JE. A novel method for the induction of experimental glaucoma using magnetic microspheres. *Invest Ophthalmol Vis Sci*. 2011;52:1671–1675.
15. Morgan JE, Tribble JR. Microbead models in glaucoma. *Exp Eye Res*. 2015;141:9–14.
16. Sappington RM, Carlson BJ, Crish SD, Calkins DJ. The microbead occlusion model: a paradigm for induced ocular hypertension in rats and mice. *Invest Ophthalmol Vis Sci*. 2009;51:207–216.
17. Cone FE, Gelman SE, Son JL, Pease ME, Quigley HA. Differential susceptibility to experimental glaucoma among 3 mouse strains using bead and viscoelastic injection. *Exp Eye Res*. 2010;91:415–424.
18. Buckingham BP, Inman DM, Lambert W, et al. Progressive ganglion cell degeneration precedes neuronal loss in a mouse model of glaucoma. *J Neurosci*. 2008;28:2735–2744.
19. Almasieh M, Wilson AM, Morquette B. Cueva Vargas JL Di Polo A. The molecular basis of retinal ganglion cell death in glaucoma. *Prog Retin Eye Res*. 2012;31:152–181.
20. Nickells RW. The cell and molecular biology of glaucoma: mechanisms of retinal ganglion cell death. *Invest Ophthalmol Vis Sci*. 2012;53:2476–2481.
21. Howell GR, Macalinao DG, Sousa GL, et al. Molecular clustering identifies complement and endothelin induction as early events in a mouse model of glaucoma. *J Clin Invest*. 2011;121:1429–1444.
22. Guo Y, Cepurna WO, Dyck JA, Doser TA, Johnson EC, Morrison JC. Retinal cell responses to elevated intraocular pressure: a gene array comparison between the whole retina and retinal ganglion cell layer. *Invest Ophthalmol Vis Sci*. 2010;51:3003–3018.
23. Guo Y, Johnson EC, Cepurna WO, Dyck JA, Doser T, Morrison JC. Early gene expression changes in the retinal ganglion cell layer of a rat glaucoma model. *Invest Ophthalmol Vis Sci*. 2011;52:1460–1473.
24. Johnson EC, Doser TA, Cepurna WO, et al. Cell proliferation and interleukin-6-type cytokine signaling are implicated by gene expression responses in early optic nerve head injury in rat glaucoma. *Invest Ophthalmol Vis Sci*. 2011;52:504–518.
25. Johnson EC, Jia L, Cepurna WO, Doser TA, Morrison JC. Global changes in optic nerve head gene expression after exposure to elevated intraocular pressure in a rat glaucoma model. *Invest Ophthalmol Vis Sci*. 2007;48:3161–3177.
26. Jia L, Cepurna WO, Johnson EC, Morrison JC. Patterns of intraocular pressure elevation after aqueous humor outflow obstruction in rats. *Invest Ophthalmol Vis Sci*. 2000;41:1380–1385.
27. Harwerth RS, Smith EL III, DeSantis L. Experimental glaucoma: perimetric field defects and intraocular pressure. *J Glaucoma*. 1997;6:390–401.
28. Kompass KS, Agapova OA, Li W, Kaufman PL, Rasmussen CA, Hernandez MR. Bioinformatic and statistical analysis of the optic nerve head in a primate model of ocular hypertension. *BMC Neurosci*. 2008;9:93.
29. Kwong JM, Vo N, Quan A, et al. The dark phase intraocular pressure elevation and retinal ganglion cell degeneration in a rat model of experimental glaucoma. *Exp Eye Res*. 2013;112:21–28.
30. Downs JC. IOP telemetry in the nonhuman primate. *Exp Eye Res*. 2015;141:91–98.
31. Li R, Liu JH. Telemetric monitoring of 24 h intraocular pressure in conscious and freely moving C57BL/6J and CBA/CaJ mice. *Mol Vis*. 2008;14:745–749.
32. Downs JC, Burgoyne CF, Seigfreid WP, Reynaud JF, Strouthidis NG, Sallee V. 24-hour IOP telemetry in the nonhuman primate: implant system performance and initial characterization of IOP at multiple timescales. *Invest Ophthalmol Vis Sci*. 2011;52:7365–7375.
33. Tehrani S, Johnson EC, Cepurna WO, Morrison JC. Astrocyte processes label for filamentous actin and reorient early within the optic nerve head in a rat glaucoma model. *Invest Ophthalmol Vis Sci*. 2014;55:6945–6952.
34. He Z, Bui BV, Vingrys AJ. Effect of repeated IOP challenge on rat retinal function. *Invest Ophthalmol Vis Sci*. 2008;49:3026–3034.
35. Bui BV, Batcha AH, Fletcher E, Wong VH, Fortune B. Relationship between the magnitude of intraocular pressure during an episode of acute elevation and retinal damage four weeks later in rats. *PLoS One*. 2013;8:e70513.
36. Sun D, Qu J, Jakobs TC. Reversible reactivity by optic nerve astrocytes. *Glia*. 2013;61:1218–1235.
37. Morrison JC, Jia L, Cepurna W, Guo Y, Johnson E. Reliability and sensitivity of the TonoLab rebound tonometer in awake Brown Norway rats. *Invest Ophthalmol Vis Sci*. 2009;50:2802–2808.
38. Jia L, Cepurna WO, Johnson EC, Morrison JC. Effect of general anesthetics on IOP in rats with experimental aqueous outflow obstruction. *Invest Ophthalmol Vis Sci*. 2000;41:3415–3419.
39. Morrison JC, Johnson EC, Cepurna WO, Funk RH. Microvasculature of the rat optic nerve head. *Invest Ophthalmol Vis Sci*. 1999;40:1702–1709.
40. Fan YY, Zhang JM, Wang H, Liu XY, Yang FH. Leukemia inhibitory factor inhibits the proliferation of primary rat astrocytes induced by oxygen-glucose deprivation. *Acta Neurobiol Exp (Wars)*. 2013;73:485–494.
41. Fuchshofer R. The pathogenic role of transforming growth factor-beta2 in glaucomatous damage to the optic nerve head. *Exp Eye Res*. 2011;93:165–169.
42. Lutjen-Drecoll E. Morphological changes in glaucomatous eyes and the role of TGFbeta2 for the pathogenesis of the disease. *Exp Eye Res*. 2005;81:1–4.
43. Schneider M, Fuchshofer R. The role of astrocytes in optic nerve head fibrosis in glaucoma. *Exp Eye Res*. 2016;142:49–55.
44. Sasaki Y, Hoshi M, Akazawa C, et al. Selective expression of Gi/o-coupled ATP receptor P2Y12 in microglia in rat brain. *Glia*. 2003;44:242–250.

45. Orr AG, Orr AL, Li XJ, Gross RE, Traynelis SF. Adenosine A(2A) receptor mediates microglial process retraction. *Nat Neurosci*. 2009;12:872–878.
46. Abbott CJ, Choe TE, Lusardi TA, Burgoyne CF, Wang L, Fortune B. Evaluation of retinal nerve fiber layer thickness and axonal transport 1 and 2 weeks after 8 hours of acute intraocular pressure elevation in rats. *Invest Ophthalmol Vis Sci*. 2014;55:674–687.
47. Morrison JC, Johnson EC, Cepurna W, Jia L. Understanding mechanisms of pressure-induced optic nerve damage. *Prog Retin Eye Res*. 2005;24:217–240.
48. Ollivier FJ, Brooks DE, Kallberg ME, et al. Time-specific intraocular pressure curves in Rhesus macaques (Macaca mulatta) with laser-induced ocular hypertension. *Vet Ophthalmol*. 2004;7:23–27.
49. Fortune B, Bui BV, Morrison JC, et al. Selective ganglion cell functional loss in rats with experimental glaucoma. *Invest Ophthalmol Vis Sci*. 2004;45:1854–1862.
50. Pease ME, Zack DJ, Berlinicke C, et al. Effect of CNTF on retinal ganglion cell survival in experimental glaucoma. *Invest Ophthalmol Vis Sci*. 2009;50:2194–2200.
51. Levkovitch-Verbin H, Quigley HA, Martin KR, et al. The transcription factor c-jun is activated in retinal ganglion cells in experimental rat glaucoma. *Exp Eye Res*. 2005;80:663–670.
52. Abbott CJ, Choe TE, Burgoyne CF, Cull G, Wang L, Fortune B. Comparison of retinal nerve fiber layer thickness in vivo and axonal transport after chronic intraocular pressure elevation in young versus older rats. *PLoS One*. 2014;9:e114546.
53. Li ZW, Liu S, Weinreb RN, et al. Tracking dendritic shrinkage of retinal ganglion cells after acute elevation of intraocular pressure. *Invest Ophthalmol Vis Sci*. 2011;52:7205–7212.
54. Hu Q, Huang C, Wang Y, Wu R. Expression of leukemia inhibitory factor in the rat retina following acute ocular hypertension. *Mol Med Rep*. 2015;12:6577–6583.
55. Cepurna WO, Kayton RJ, Johnson EC, Morrison JC. Age related optic nerve axonal loss in adult Brown Norway rats. *Exp Eye Res*. 2005;80:877–884.
56. Zhi Z, Cepurna W, Johnson E, Jayaram H, Morrison J, Wang RK. Evaluation of the effect of elevated intraocular pressure and reduced ocular perfusion pressure on retinal capillary bed filling and total retinal blood flow in rats by OMAG/OCT. *Microvasc Res*. 2015;101:86–95.
57. Cherian L, Chacko G, Goodman JC, Robertson CS. Cerebral hemodynamic effects of phenylephrine and L-arginine after cortical impact injury. *Crit Care Med*. 1999;27:2512–2517.
58. Bui BV, Edmunds B, Cioffi GA, Fortune B. The gradient of retinal functional changes during acute intraocular pressure elevation. *Invest Ophthalmol Vis Sci*. 2005;46:202–213.
59. Chi OZ, Wei HM, Tse J, Klein SL, Weiss HR. Cerebral microregional oxygen balance during chronic versus acute hypertension in middle cerebral artery occluded rats. *Anesth Analg*. 1996;82:587–592.
60. Zhi Z, Cepurna W, Johnson E, Shen T, Morrison J, Wang RK. Volumetric and quantitative imaging of retinal blood flow in rats with optical microangiography. *Biomed Opt Express*. 2011;2:579–591.
61. Zhi Z, Cepurna WO, Johnson EC, Morrison JC, Wang RK. Impact of intraocular pressure on changes of blood flow in the retina, choroid, and optic nerve head in rats investigated by optical microangiography. *Biomed Opt Express*. 2012;3:2220–2233.
62. He Z, Nguyen CT, Armitage JA, Vingrys AJ, Bui BV. Blood pressure modifies retinal susceptibility to intraocular pressure elevation. *PLoS One*. 2012;7:e31104.
63. Holcombe DJ, Lengefeld N, Gole GA, Barnett NL. The effects of acute intraocular pressure elevation on rat retinal glutamate transport. *Acta Ophthalmol*. 2008;86:408–414.
64. Frishman LJ, Shen FF, Du L, et al. The scotopic electroretinogram of macaque after retinal ganglion cell loss from experimental glaucoma. *Invest Ophthalmol Vis Sci*. 1996;37:125–141.
65. Bui BV, Fortune B. Ganglion cell contributions to the rat full-field electroretinogram. *J Physiol*. 2004;555:153–173.
66. Fortune B, Choe TE, Reynaud J, et al. Deformation of the rodent optic nerve head and peripapillary structures during acute intraocular pressure elevation. *Invest Ophthalmol Vis Sci*. 2011;52:6651–6661.
67. Dai C, Khaw PT, Yin ZQ, Li D, Raisman G, Li Y. Structural basis of glaucoma: the fortified astrocytes of the optic nerve head are the target of raised intraocular pressure. *Glia*. 2012;60:13–28.
68. Huang XR, Knighton RW. Altered F-actin distribution in retinal nerve fiber layer of a rat model of glaucoma. *Exp Eye Res*. 2009;88:1107–1114.
69. WoldeMussie E, Ruiz G, Wijono M, Wheeler LA. Neuroprotection of retinal ganglion cells by brimonidine in rats with laser-induced chronic ocular hypertension. *Invest Ophthalmol Vis Sci*. 2001;42:2849–2855.
70. Mabuchi F, Aihara M, Mackey MR, Lindsey JD, Weinreb RN. Regional optic nerve damage in experimental mouse glaucoma. *Invest Ophthalmol Vis Sci*. 2004;45:4352–4358.
71. Pazos M, Yang H, Gardiner SK, et al. Rat optic nerve head anatomy within 3D histomorphometric reconstructions of normal control eyes. *Exp Eye Res*. 2015;139:1–12.
72. Heinrich PC, Behrmann I, Haan S, Hermanns HM, Muller-Newen G, Schaper F. Principles of interleukin (IL)-6-type cytokine signalling and its regulation. *Biochem J*. 2003;374:1–20.
73. Buono KD, Goodus MT, Guardia Clausi M, Jiang Y, Loporchio D, Levison SW. Mechanisms of mouse neural precursor expansion after neonatal hypoxia-ischemia. *J Neurosci*. 2015;35:8855–8865.
74. McPherson CA, Aoyama M, Harry GJ. Interleukin (IL)-1 and IL-6 regulation of neural progenitor cell proliferation with hippocampal injury: differential regulatory pathways in the subgranular zone (SGZ) of the adolescent and mature mouse brain. *Brain Behav Immun*. 2011;25:850–862.
75. Mi H, Haeberle H, Barres BA. Induction of astrocyte differentiation by endothelial cells. *J Neurosci*. 2001;21:1538–1547.
76. Uemura A, Takizawa T, Ochiai W, Yanagisawa M, Nakashima K, Taga T. Cardiotrophin-like cytokine induces astrocyte differentiation of fetal neuroepithelial cells via activation of STAT3. *Cytokine*. 2002;18:1–7.
77. Emery B, Cate HS, Marriott M, et al. Suppressor of cytokine signaling 3 limits protection of leukemia inhibitory factor receptor signaling against central demyelination. *Proc Natl Acad Sci U S A*. 2006;103:7859–7864.
78. Karmarkar SW, Bottum KM, Tischkau SA. Considerations for the use of anesthetics in neurotoxicity studies. *Comp Med*. 2010;60:256–262.
79. Xiao Z, Ren P, Chao Y, et al. Protective role of isoflurane pretreatment in rats with focal cerebral ischemia and the underlying molecular mechanism. *Mol Med Rep*. 2015;12:675–683.
80. Burchell SR, Dixon BJ, Tang J, Zhang JH. Isoflurane provides neuroprotection in neonatal hypoxic ischemic brain injury. *J Investig Med*. 2013;61:1078–1083.

Investigative Ophthalmology & Visual Science